

# Piecemeal Quantum Telescope: Exponential Precision with Super Robustness and Efficiency

Jian Leng,<sup>1</sup> Yi-Xin Shen,<sup>1</sup> Zhou-Kai Cao,<sup>1</sup> and Xiang-Bin Wang<sup>1,2,3,4,\*</sup>

<sup>1</sup>*State Key Laboratory of Low Dimensional Quantum Physics, Department of Physics, Tsinghua University, Beijing 100084, China*

<sup>2</sup>*Jinan Institute of Quantum Technology and Jinan branch, Hefei National Laboratory, Jinan, Shandong 250101, China*

<sup>3</sup>*International Quantum Academy, Shenzhen 518048, China*

<sup>4</sup>*Frontier Science Center for Quantum Information, Beijing 100193, China*

We propose the piecemeal quantum telescope through bit-by-bit iteration using different baselines. It improves precision exponentially with number of baselines, and it works robustly under large observation errors such as statistical errors, channel noise, operational errors and so on. For example, under the noisy channel of random phase drifts, our method can provide an exponential precision provided that the detected data is not entirely noisy. Being fault tolerant to statistical error, it requests only a small number of incident single-photons in detecting the star angle with exponential precision. As a result, it requests to detect only a few hundreds of photons from the target star for a precision breaking classical limit by 4 to 5 magnitude orders. This demonstrates a super efficiency.

## I. INTRODUCTION

Quantum imaging can be used to obtain more information than classical imaging by applying quantum interferometry [1–11]. Especially, quantum telescopes [1–4] can detect more precise angle value of single-star target than classical telescope. However, the light from a remote source is disturbed and attenuated in transmitting atmosphere before arriving at ground. Therefore it is meaningful to investigate robust and efficient method which can detect the angle value precisely with a large observation error or with a small number of incident single-photons. The precision of existing quantum telescopes has been improved in the scale of square root of incident single photons [1–11]. Here we propose the piecemeal quantum telescope which uses  $K$  baselines, reaching an exponential precision whose uncertainty is proportional to  $(1/2)^K$ . However, in each individual baseline, our method only requests the observed data in a large range, allowing a fairly large observation error. This leads to strong fault tolerance property for our method. For example, under the noisy channel of random phase drifts, our method can provide an exponential precision provided that the detected data is not entirely noisy. Surely, the fault tolerant property is not only limited to channel noise, it also works for large statistical error due to small data size. Given this fact, our method presents a high precision breaking the classical limit by several magnitude orders while requesting to detect only a few hundreds of single-photons from the target star.

## II. OUR METHOD IN SIMPLIFIED MODEL

The proposed set-up of our piecemeal quantum telescope is schematically shown in Fig. 1. There are  $K + 1$  baselines and we collect data from each of them. The

length of baseline  $k$  is  $L_k$ , where  $k = \{0, 1, \dots, K\}$ . For ease of presentation, at this moment we consider a simplified model only, ignoring the reference source and taking simple relation of  $L_k = 2^k L_0$ . Later in this manuscript, we shall take further studies with realistic conditions such as using reference star in Sec. III, the more general relation for  $\{L_k\}$  in Sec. VI. Suppose that the target source is a single star with a small angle  $\theta$  as shown in Fig. 1(a). The state single photon arriving at two receivers of pair

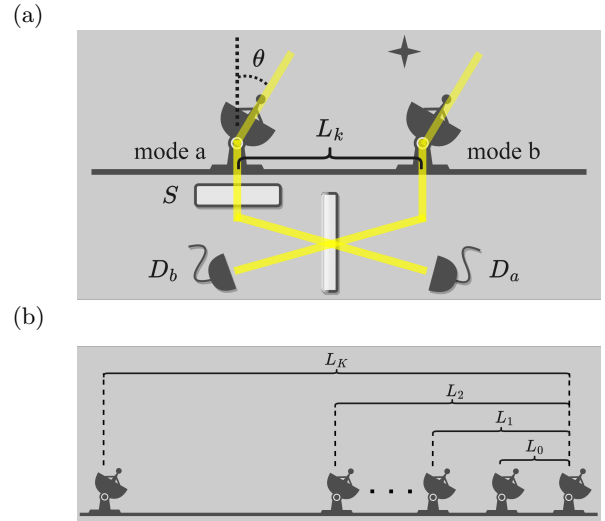


FIG. 1. Schematic setup of our method: it contains different baselines  $\{L_k\}$ . (a) Collecting data from a pair of receivers (telescopes) with phase shifter  $S$ , 50:50 beam splitter, threshold detectors  $D_a$  and  $D_b$ . (b) In each iteration, it collects data from a pair of telescopes on each individual baseline  $L_k$ , and then process the data jointly by Eq. (3) (or Eq. (8)). Our method requests different baseline lengths only. A realization is not limited to schematic Fig. (b) above. For example, we can choose to use two independent telescopes for each individual baselines and hence can take observations at all baselines simultaneously.

$k$  is

$$|\mathcal{S}_k\rangle = \frac{1}{\sqrt{2}}(|01\rangle + e^{i\phi_k}|10\rangle), \quad \phi_k \approx 2\pi \frac{L_k}{\lambda} \theta. \quad (1)$$

Here  $\lambda$  is the wavelength,  $|c_a c_b\rangle$  represents photon numbers of mode  $a$  and  $b$  and  $\phi_0 \in [0, 2\pi)$ . We set zero and  $\frac{\pi}{2}$  phase shifts of  $S$  to collect the first and second set of data, respectively. We set  $L_k = (\frac{1}{2})^k L_0$  at this moment and derive our calculation formula Eq. (3) with this setting. Latter, through similar derivation, we shall present the calculation formula in Eq. (17) with more general mathematical setting of baseline length  $L_{k+1} = s_k L_k$  latter.

We start with some mathematical notations.

- 1) Taking  $L_k = 2^k L_0$  and hence  $\phi_{k+1} = 2\phi_k$ .
- 2)  $\hat{x} = x \bmod 2\pi$ . When using  $\alpha \cdot \hat{x}$ , we mean  $\alpha \cdot (x \bmod 2\pi)$ .
- 3)  $\hat{\phi}_k$ : The observed value of  $\phi_k$ . In our setup  $\hat{\phi}_k$  is obtained based on the experimentally collected data. Details are shown around Eq. (11) in Sec. III.

In our calculation below we introduce a new variable

$$\psi_k = \phi_k - \hat{\phi}_k + \pi,$$

and its modulo

$$\hat{\psi}_k = (\phi_k - \hat{\phi}_k + \pi) \bmod 2\pi.$$

The definition of  $\psi_k$  means  $\psi_{k+1} = \phi_{k+1} - \hat{\phi}_{k+1} + \pi$ . As shown in the Sec. I of Supplementary Material [12], the following equation

$$2 \cdot \hat{\psi}_k = \hat{\psi}_{k+1} + \hat{r}_{k+1} \quad (2)$$

can hold with a small failure probability, because the failure case requests very large observation error. Here  $r_{k+1} = \hat{\phi}_{k+1} - 2\hat{\phi}_k + \pi$ . Using Eq. (2) iteratively we obtain

$$\hat{\psi}_0 = \sum_{k=1}^K \left(\frac{1}{2}\right)^k \hat{r}_k + \left(\frac{1}{2}\right)^K \hat{\psi}_K.$$

Recalling the definition  $\hat{\psi}_0 = (\phi_0 - \hat{\phi}_0 + \pi) \bmod 2\pi$  and taking the approximation  $\hat{\psi}_K = \pi$ , we obtain

$$\hat{\phi}_0 = \left( \hat{\phi}_0 - \pi + \sum_{k=1}^K \left(\frac{1}{2}\right)^k \hat{r}_k + \left(\frac{1}{2}\right)^K \pi \right) \bmod 2\pi. \quad (3)$$

Since we have requested  $\phi_0 \in [0, 2\pi)$  earlier, here  $\hat{\phi}_0 = \hat{\phi}_0$ . Since  $(\frac{1}{2})^k$  represents  $k$ th binary bit after the decimal point, we see a bit-by-bit iteration behavior in the term  $\sum_{k=1}^K (\frac{1}{2})^k \hat{r}_k$  with the summation direction  $k$  from  $K$  to 1.

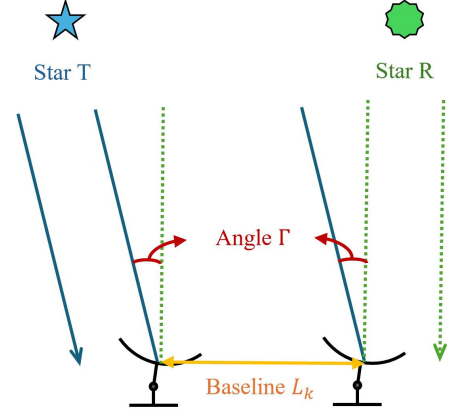


FIG. 2. Using a reference star with a known position can help reduce the failure probability inherent to the experimental devices. For each baseline length  $L_k$ , photons from both the target star and the reference star are received and the experimental data are processed jointly, as shown in Eq. (8).

### III. OUR METHOD WITH MORE REALISTIC CONDITIONS

Consider two remote sources or two stars: the reference star R and the target star T. Our goal is to detect the angle of star T relative to star R, i.e., angle  $\Gamma$  in Fig. 2. The value of  $\Gamma$  can be around the magnitude order of 1 arcsecond. Suppose we have some crude information about angle  $\Gamma$  and we write it in the following form:

$$\Gamma = \Gamma_0 + \theta_T \quad (4)$$

where  $\Gamma_0$  is an exact value known to us while  $\theta_T$  is an unknown small value whose range is  $\theta_T \in [0, \theta_0]$ , value  $\theta_0$  is known precisely. The value of  $\Gamma_0$  can be around 1 arcsecond or several arcseconds, while the value of  $\theta_0$  can be around magnitude of 1 milliarcsecond. Therefore we can distinguish incident photons from different stars and hence can perform the interference experiment for photons from different stars separately. We denote  $\Phi_{T,k}$  and  $\Phi_{R,k}$  for phase difference of incident light to telescopes at baseline  $k$  from star T and R, respectively. In particular,

$$\begin{aligned} \Phi_{R,k} &= \frac{2\pi L_k}{\lambda} \sin \theta_R \\ \Phi_{T,k} &= \frac{2\pi L_k}{\lambda} \sin (\Gamma + \theta_R) \\ &= \frac{2\pi L_k}{\lambda} \sin (\Gamma_0 + \theta_T + \theta_R), \end{aligned} \quad (5)$$

where  $\theta_R$  (or  $\Gamma + \theta_R$ ) is the angle between baseline  $k$  and wave plane of light from star R (or wave plane of light from star T).

In our setup, the baselines are supposed to be (almost) parallel to each other and parallel to plane TOR. Here O is any point around the telescopes. (If the sources are

remote stars T and R, we can simply regard the earth as point O.) The baselines are also supposed to be (almost) orthogonal to wave ray of light from star R. This means  $\theta_R \sim 0$ . The difference of phase difference is

$$\Phi_{T,k} - \Phi_{R,k} = \frac{2\pi L_k \sin \Gamma}{\lambda}$$

Taking the conditions that  $\theta_R \sim 0$ ,  $\Gamma_0$  around arcseconds, we have

$$\Phi_{T,k} - \Phi_{R,k} \approx \frac{2\pi L_k}{\lambda} (\sin \Gamma_0 + \cos \Gamma_0 \sin \theta_T).$$

Denoting

$$\frac{2\pi L_k}{\lambda} \cos \Gamma_0 \sin \theta_T = \Delta_k, \quad (6)$$

we have

$$\Delta_k = \Phi_{T,k} - \Phi_{R,k} - \frac{2\pi L_k}{\lambda} \sin \Gamma_0, \quad (7)$$

which can be observed experimentally because values of terms at the right side of the Eq. (7) are either experimentally observable or exactly known.

Denoting  $\Psi_k = \Delta_k - \hat{\Delta}_k + \pi$ ,  $\dot{\gamma}_k = (\hat{\Delta}_k - 2\hat{\Delta}_{k-1} + \pi) \bmod 2\pi$  and taking the iterations and derivation similar to those used for Eq. (2), we obtain

$$\hat{\Delta}_0 = \left( \hat{\Delta}_0 - \pi + \sum_{k=1}^K \left(\frac{1}{2}\right)^k \dot{\gamma}_k + \left(\frac{1}{2}\right)^K \pi \right) \bmod 2\pi \quad (8)$$

It is just  $\Delta_0$  if we set  $L_0 \sin \theta_0 < 2\pi$ . By Eq. (8), we can calculate  $\theta_T$  according to Eq. (6) with  $k = 0$ . Eq. (3) and Eq. (8) are the main calculation formulas of our method of piecemeal telescope.

#### IV. FAULT TOLERANCE PROPERTIES

Consider our simplified model with Eq. (3) first. On the one hand, our method reaches an exponential precision whose uncertainty comes from replacing the term  $(\frac{1}{2})^K \dot{\psi}_K$  by  $(\frac{1}{2})^K \pi$ , which means an exponentially small value proportional to  $(\frac{1}{2})^K$ . On the other hand, our method does not request a precise observed value for each individual baseline. Actually, the condition of Eq. (2) allows fairly large observation error[12]. As a simple example, a sufficient condition for Eq. (2) is that the observed value resides in the same quadrant with the exact value for  $k$  and  $k + 1$ .

**Fact 1:** Our method works exactly provided that the observed value  $\{\hat{\phi}_k\}$  is in the same quadrant with the exact value  $\{\phi_k\}$  for all  $k$ .

Consider the 50:50 beamsplitter setup in Fig. 1(a). We shall use the observed number of counts of each of the two detectors. Here we only consider the asymptotic

case. In the experiment of each  $L_k$ , two data sets of observed data (number of counts of each selector) are collected, i.e., setting phase shift of S being 0 for the first data set, and  $\pi/2$  for the second data set.

Suppose in the noiseless case, the first data set is  $(n_l, n_r)$  and the second data set is  $(n'_l, n'_r)$ , where  $n_l$  ( $n_r$ ) and  $n'_l$  ( $n'_r$ ) are the number of counts at left (right) detector in each data set. In flipping error model, the observed values of counts at each detectors of the first data set (with phase-shift of S being set 0) are:

$$\begin{cases} \hat{n}_l = n_l(1 - p_l) + n_r p_r \\ \hat{n}_r = n_r(1 - p_r) + n_l p_l. \end{cases} \quad (9)$$

where  $p_l$ ,  $p_r$  are flipping rates. Similar equation also holds for the second data set (with phase-shift of S being set  $\pi/2$ ):

$$\begin{cases} \hat{n}'_l = n'_l(1 - p'_l) + n'_r p'_r \\ \hat{n}'_r = n'_r(1 - p'_r) + n'_l p'_l. \end{cases} \quad (10)$$

where  $p'_l$ ,  $p'_r$  are flipping rates, and  $\hat{n}'_l$  and  $\hat{n}'_r$  are the observed values of counts at each detectors of the second data set. With these we can determine the values of  $\{\hat{\phi}_k\}$  and  $\{\hat{\phi}'_k\}$  exactly by formulas of beamsplitter interference, as shown in Sec.V. Here in this section we only need to know the specific quadrant of  $\{\hat{\phi}_k\}$  (and  $\{\hat{\phi}'_k\}$ ), which are determined by the following fact:

**Fact 2:** For any  $k$ , the quadrant of  $\hat{\phi}_k$  is determined by signs of  $n_l - n_r$  and  $n'_l - n'_r$ , and the quadrant of  $\hat{\phi}'_k$  is determined by  $\hat{n}_l - \hat{n}_r$  and  $\hat{n}'_l - \hat{n}'_r$ .

It is to say that, the flipping error model given by Eq. (9) and Eq. (10) does not change the sign of any difference term  $x - y$  as appeared in **Fact 2** above if all flipping rates are less than 50%. Therefore the observed value  $\hat{\phi}_k(\hat{\phi}'_k)$  and the exact value  $\phi_k(\phi'_k)$  are in the same quadrant provided that all flipping rates are less than 50%.

Obviously, all discussions above also hold for our method with Eq. (8). We conclude:

*Theorem 1:* Asymptotically, our method with Eq. (3) and our method with Eq. (8) can work exactly with flipping errors if the flipping rates are less than 50%.

As a direct application we have the following corollary:

*Corollary 1:* Asymptotically, our method with Eq. (3) and our method with Eq. (8) can work exactly under any noisy channel of random phase drifts in the range of  $[-\delta, \delta]$ , provided that  $0 \leq \delta < \pi$ .

*Theorem 1* and *Corollary 1* actually show that our method can reach exponential precision under large noise if the observed data is not entirely noisy. Our numerical simulation confirmed this, see in Fig. 3.

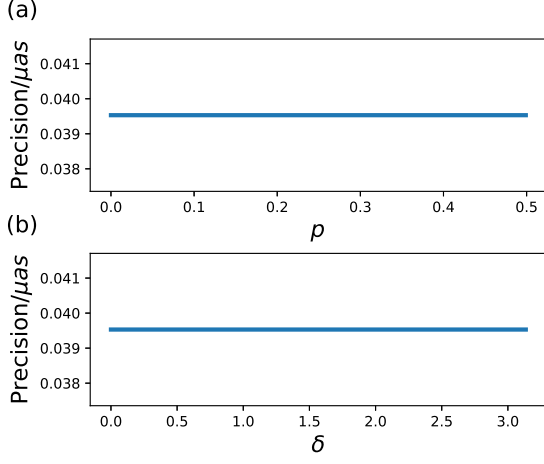


FIG. 3. The precision of our method with observation error. The precision is defined as  $\hat{\theta}_T - \theta_T$ , where  $\theta_T$  is the value obtained by our method with Eq. (8) and  $\theta_T$  is the exact value. We have taken  $K + 1 = 15$  baselines. (a) Result with flipping error model of flipping rate  $p_l = p_r = p'_l = p'_r = p$ . (b) Result under noisy channel with random phase drifts between  $[-\delta, \delta]$ .

## V. SUPER PRECISION WITH SMALL DATA SIZE AND NUMERICAL SIMULATIONS

Surely, the fault tolerance property of our method can also apply to the observation error from large statistical fluctuation due to small data size. We study this issue here and as a result, we demonstrate the super efficiency of our method numerically: exponential precision with small data size from the target star.

To do calculation by Eq. (3), we need the observed values  $\{\hat{\phi}_k | k = 0, 1, \dots, K\}$  as the input. In our calculation, we can produce these values based on experimental data. In our proposed set-up Fig. 1, we shall collect two sets of data. The first (second) set is obtained through setting zero ( $\frac{\pi}{2}$ ) phase shift on  $S$ . In the first (second) set, we observe the event of detector  $D_a$  silent and  $D_b$  clicking for  $m_k$  ( $\bar{m}_k$ ) times in total detected events of one-detector-clicking  $M_k$  ( $\bar{M}_k$ ). We have

$$\hat{\phi}_k = \frac{1}{2} (\cos^{-1} q_k + \sin^{-1} \bar{q}_k) \bmod 2\pi, \quad (11)$$

where

$$q_k = 1 - \frac{2m_k}{M_k}, \quad \bar{q}_k = \frac{2\bar{m}_k}{\bar{M}_k} - 1. \quad (12)$$

In this work, we shall only consider the important practical issue of small data size with possible statistical errors but we assume perfect devices. For imperfect devices, see Section II of Supplementary Material [12].

Since  $M_k$  and  $\bar{M}_k$  are finite number in practical detection, the  $\phi_0$  value calculated by Eq. (3) does not exactly

equal to the actual value of  $\phi_0$ . Denoting  $\tilde{\phi}_0$  as the  $\phi_0$  value calculated by Eq. (3), we define the failure probability  $\epsilon$  as

$$\epsilon = P(|\tilde{\phi}_0 - \phi_0| > \frac{\pi}{2^{K+1}}). \quad (13)$$

This gives the precision of our piecemeal method

$$\delta\phi = \frac{\pi}{2^{K+1}}, \quad \delta\theta = \frac{\lambda}{2\pi L_0} \delta\phi = \frac{\lambda}{4L}. \quad (14)$$

In our numerical simulation, we first generate a set of ‘experimental data’  $\{m_k, \bar{m}_k\}$ , according to the probability distributions  $P(m_k | M_k)$  and  $P(\bar{m}_k | \bar{M}_k)$  given by known phase value  $\phi_0$ . They obey Binomial distributions

$$\begin{aligned} P(m_k | M_k) &= C_{M_k}^{m_k} p_k^{m_k} (1 - p_k)^{M_k - m_k}, \\ P(\bar{m}_k | \bar{M}_k) &= C_{\bar{M}_k}^{\bar{m}_k} \bar{p}_k^{\bar{m}_k} (1 - \bar{p}_k)^{\bar{M}_k - \bar{m}_k}, \end{aligned} \quad (15)$$

For the simplified model  $p_k = \frac{1}{2}(1 - \cos 2^k \phi_0)$  and  $\bar{p}_k = \frac{1}{2}(1 + \sin 2^k \phi_0)$  are fixed for the baseline  $L_k$ . Using  $\{m_k, \bar{m}_k\}$ , we calculate the estimated value  $\tilde{\phi}_0$  of the simplified model by Eq. (3). If  $|\tilde{\phi}_0 - \phi_0| < \delta\phi$ , we regard it as a successful event otherwise a failure event. Repeating it many times, we calculate the ratio of number of failure events and the total number of events which gives the failure probability  $\epsilon$ . We take simulations for many different  $\phi_0$  values from 0 to  $2\pi$ . To quantify the performance, all  $\{M_k, \bar{M}_k\}$  are taken as the same value  $M$  and we set  $K = 14$ . Numerical results for  $M = 1, 4$  and 7 are shown in Fig. 4. We take  $M = 7$  in following discussions.

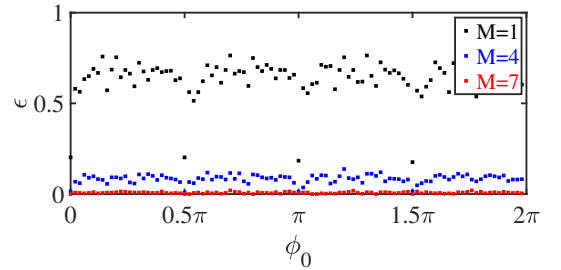


FIG. 4. The failure probability  $\epsilon$  changes with  $\phi$  for detecting single-star target. We take  $M_k = \bar{M}_k = M$  for every  $k$ . For the red data points in the figure, we assume the number of detected photons is  $2 \times 7 = 14$  for each baseline and the total number of detected photons is  $14(K+1) = 210$ , and the failure probability for this case is around 0.0073, less than 1%. Each data point is obtained by averaging 500 samples. The failure probability is defined by Eq. (13), pointing to an exponential precision with uncertainty  $\frac{\pi}{2^{15}}$ .

If we use quantum memory with error correction [3], we do not have to consider photon loss in transmission from each receivers. Therefore the total number of single-photons at receives is  $M_t = 2M(K + 1)$ . Applying Eq.

(14), we have  $\delta\theta = \frac{\lambda}{2L_0} 2^{-\frac{M_t}{2M}} \propto 2^{-M_t}$ . Numerical simulation of the performance of our method is shown in Fig. 5(a), where we have taken comparison with classical telescope  $\delta\theta_c$  (Hubble Space Telescope, diameter  $D = 2.4\text{m}$ ) and existing quantum telescopes  $\delta\theta_Q$  [1–4]. In the calculation, we take  $M = 7$  and  $\lambda = 628\text{nm}$ . For a fair comparison, we assume the same initial crude information of angle range  $(0, \theta_{\max})$  for both the existing quantum telescopes and our method. We take  $\theta_{\max} = 10\text{mas}$  and obtain  $L_0 \approx \frac{\lambda}{\theta_{\max}} = 13\text{m}$  from Eq. (1). Calculation details for classical telescope and existing quantum telescopes are shown in Section III in Supplementary Material [12]. Now we consider the performance

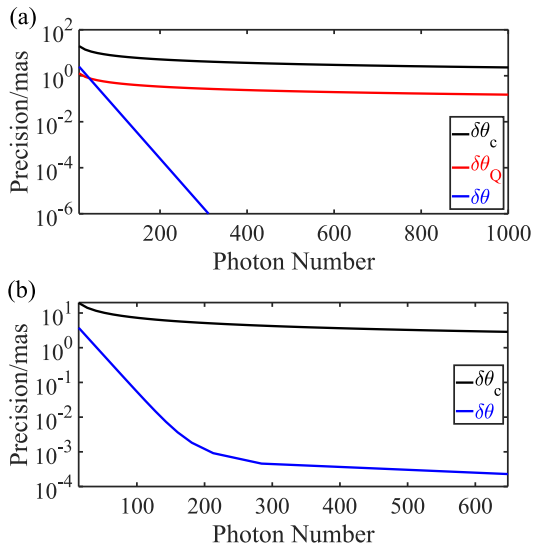


FIG. 5. Precisions of Hubble Space Telescope  $\delta\theta_c$ , existing quantum telescope  $\delta\theta_Q$  and our piecemeal quantum telescope  $\delta\theta$  for detecting single-star target. The horizontal axis is the total number  $M_t$  of incident single-photons to receivers. (a) Using quantum memory for  $\delta\theta_Q$  and  $\delta\theta$ . (b) Not using quantum memory. Our proposed piecemeal quantum telescope reaches the observation precision within the uncertainty of  $\theta = 10^{-3}\text{mas}$  requesting about 212 received photons (totally 182 detected photons in  $K + 1 = 14$  baselines).

without quantum memory. The channel transmittance is  $\eta(l)$  of optical fiber of length  $l$ . We need the baseline of length  $L_k = 2^k L_0$  for pair  $k$ . Suppose that beam splitter locates at the middle of fiber. The transmittance of optical fiber is  $\eta(2^{k-1}L_0)$ . The incident single-photons at receivers have a probability  $\eta(2^{k-1}L_0)$  to arrive at detectors. So the total number of collected single-photons at receivers is  $M_t = \sum_{k=0}^K \frac{2M}{\eta(2^{k-1}L_0)}$ . Applying Eq. (14), we can obtain a relation between precision and total photon number  $\delta\theta(M_t)$ . We compare our result with Hubble Space Telescope  $\delta\theta_c$  in Fig. 5(b). We take standard optical fiber, that is  $\eta(l) = 10^{(-\alpha L/10)}$  where  $\alpha = 0.2$  and  $l_0 = 10\text{km}$ . We set  $M = 7$ ,  $\theta_{\max} = 15\text{mas}$  and obtain  $L_0 \approx \frac{\lambda}{\theta_{\max}} = 8.6\text{m}$  from Eq. (1). When  $\delta\theta \approx 10^{-3}\text{mas}$ , we have  $K = 13$  then the length of fiber

is  $2^{K-1}L_0 \approx 35\text{km}$  that is feasible for practical application.

## VI. MORE GENERAL FORMULA

In Sec. II, we have shown how to detect the single-star target with the baseline  $L_k = 2^k L_0$ . It is easy to extend the method for more general case that  $L_{k+1} = s_k L_k$ , where integer  $s_k$  can take different value for different  $k$ . Directly, we have  $\phi_{k+1} = s_k \phi_k$ . Similar to Sec. II, we introduce a new variable

$$\psi_k = \phi_k - \hat{\phi}_k + \pi,$$

and its modulo

$$\dot{\psi}_k = (\phi_k - \hat{\phi}_k + \pi) \bmod 2\pi.$$

One can follow the similar proof of Sec. I in Supplementary Material [12], and obtain that the following equation

$$s_k \cdot \dot{\psi}_k = \dot{\psi}_{k+1} + \dot{r}_{k+1} + (s_k - 2)\pi. \quad (16)$$

can hold with a small failure probability if the observation error is not too large. Here  $r_{k+1} = \hat{\phi}_{k+1} - s_k \hat{\phi}_k + \pi$ . In particular, taking  $s_k = 2$  in Eq. (16) we obtain the formula in Eq. (2). Using Eq. (16) iteratively we have

$$\begin{aligned} \dot{\psi}_0 &= \prod_{r=0}^{K-1} \left( \frac{1}{s_r} \right) \left( \sum_{i=1}^{K-1} \prod_{j=i}^{K-1} s_j \dot{r}_i + \dot{r}_K + \dot{\psi}_K \right) \\ &+ \sum_{i=0}^{K-2} \prod_{j=i+1}^{K-1} (s_i - 2) s_j \pi + (s_{K-1} - 2)\pi \\ &= L_0 \left( \sum_{i=1}^K \frac{\dot{r}_i}{L_i} + \frac{\dot{\psi}_K}{L_K} + \sum_{i=0}^{K-1} \frac{(s_i - 2)\pi}{L_{i+1}} \right) \end{aligned} \quad (17)$$

where  $\prod_{j=0}^{i-1} s_j = L_i/L_0$  has been used. Recalling the definition  $\dot{\psi}_0 = (\phi_0 - \hat{\phi}_0 + \pi) \bmod 2\pi$  and taking the approximation  $\dot{\psi}_K = \pi$ , we obtain

$$\phi_0 = \left( \dot{\psi}_0 + \hat{\phi}_0 - \pi \right) \bmod 2\pi,$$

with  $\dot{\psi}_0$  given by Eq. (17).

## VII. CONCLUSION

We propose an efficient method of quantum telescope using different baseline lengths through bit-by-bit iteration. The exponential precision for our method requests only a small number of detected photons. It works with large noise provided that the detected result is not entirely noisy.

We acknowledge the financial support in part by National Natural Science Foundation of China grant

No.11974204 and No.12174215, and Innovation Program for Quantum Science and Technology No. 2021ZD0300705. This study is also supported by the Taishan Scholars Program. We thank Prof. Y Cao of USTC for useful discussions.

---

\* xbwang@mail.tsinghua.edu.cn

- [1] D. Gottesman, T. Jennewein, and S. Croke, Longer-baseline telescopes using quantum repeaters, *Physical review letters* **109**, 070503 (2012).
- [2] E. T. Khabiboulline, J. Borregaard, K. De Greve, and M. D. Lukin, Optical interferometry with quantum networks, *Physical review letters* **123**, 070504 (2019).
- [3] Z. Huang, G. K. Brennen, and Y. Ouyang, Imaging stars with quantum error correction, *Physical Review Letters* **129**, 210502 (2022).
- [4] M. M. Marchese and P. Kok, Large baseline optical imaging assisted by single photons and linear quantum optics, *Physical Review Letters* **130**, 160801 (2023).
- [5] U. Zanforlin, C. Lupo, P. W. Connolly, P. Kok, G. S. Buller, and Z. Huang, Optical quantum super-resolution imaging and hypothesis testing, *Nature Communications* **13**, 5373 (2022).
- [6] L. Howard, G. Gillett, M. Pearce, R. Abrahao, T. Weinhold, P. Kok, and A. White, Optimal imaging of remote bodies using quantum detectors, *Physical review letters* **123**, 143604 (2019).
- [7] C. Lupo, Z. Huang, and P. Kok, Quantum limits to incoherent imaging are achieved by linear interferometry, *Physical Review Letters* **124**, 080503 (2020).
- [8] Z. Huang and C. Lupo, Quantum hypothesis testing for exoplanet detection, *Physical Review Letters* **127**, 130502 (2021).
- [9] Y. Wang, Y. Zhang, and V. O. Lorenz, Superresolution in interferometric imaging of strong thermal sources, *Physical Review A* **104**, 022613 (2021).
- [10] Z. Chen, A. Nomerotski, A. Slosar, P. Stankus, and S. Vintskevich, Astrometry in two-photon interferometry using an earth rotation fringe scan, *Physical Review D* **107**, 023015 (2023).
- [11] Z. Huang, C. Schwab, and C. Lupo, Ultimate limits of exoplanet spectroscopy: A quantum approach, *Physical Review A* **107**, 022409 (2023).
- [12] Supplementary material for ‘piecemeal quantum telescope with superresolution’.

## Supplementary Material for ‘Piecemeal Quantum Telescope with Super Efficiency’

### I. Mathematical derivation of iteration formula

Consider the formula below that relates the actual value  $\hat{\phi}_k$  and its observed value  $\hat{\phi}_k$

$$\hat{\phi}_k = (\hat{\phi}_k + e_k) \bmod 2\pi, \text{ for any } k,$$

where  $e_k \in (-\pi, \pi]$  can be regarded as the error of the observation.

Define  $r_{k+1} = \hat{\phi}_{k+1} - 2\hat{\phi}_k + \pi$ . For the equation

$$Z_k = 2 \cdot \hat{\psi}_k - \hat{\psi}_{k+1} - \hat{r}_{k+1},$$

consider the conditions:

$$\begin{cases} |e_k| < \pi, \\ |e_{k+1}| < \pi, \\ |e_{k+1} - 2e_k| < \pi. \end{cases}$$

Under these conditions, we demonstrate that  $Z_k = 0$ .

**Proof:** Observe the identity in modulo arithmetic:

$$(x \bmod 2\pi + y) \bmod 2\pi = (x + y) \bmod 2\pi.$$

Applying this identity, we derive the following:

$$\begin{aligned} 2 \cdot \hat{\psi}_k &= 2[(\hat{\phi}_k - (\hat{\phi}_k + e_k) \bmod 2\pi + \pi) \bmod 2\pi] \\ &= 2\pi - 2e_k, \\ \hat{\psi}_{k+1} &= (\hat{\phi}_{k+1} - (\hat{\phi}_{k+1} + e_{k+1}) \bmod 2\pi + \pi) \bmod 2\pi \\ &= \pi - e_{k+1}, \\ \hat{r}_{k+1} &= ((\hat{\phi}_{k+1} + e_{k+1}) \bmod 2\pi - 2(\hat{\phi}_k + e_k) \bmod 2\pi + \pi) \\ &\quad \bmod 2\pi \\ &= ((\hat{\phi}_{k+1} - 2(\hat{\phi}_k)) \bmod 2\pi + e_{k+1} - 2e_k + \pi) \bmod 2\pi. \end{aligned}$$

Given  $\hat{\phi}_{k+1} = (2 \cdot \hat{\phi}_k) \bmod 2\pi$ , it follows that:

$$(\hat{\phi}_{k+1} - 2 \cdot \hat{\phi}_k) \bmod 2\pi = 0.$$

Consequently,

$$\hat{r}_{k+1} = (e_{k+1} - 2e_k + \pi) \bmod 2\pi = e_{k+1} - 2e_k + \pi.$$

Hence,

$$\begin{aligned} Z_k &= 2 \cdot \hat{\psi}_k - \hat{\psi}_{k+1} - \hat{r}_{k+1} \\ &= 2\pi - 2e_k - (\pi - e_{k+1}) - (e_{k+1} - 2e_k + \pi) = 0. \quad \square \end{aligned}$$

From this we see that the event with  $Z_k \neq 0$  is very unlikely because it can only happens with large errors of observed values. Statistically, errors of observed values decrease rapidly with the rise of data size. Numerical simulation in Fig. 2 shows that a few detected photons can compress the failure probability to less than 1% for a high precision  $\frac{\pi}{256}$  of the result calculated by our Eq. (3).

### II. Collecting data with practical devices and weak incident light

Suppose the weak incident light contains a single photon with probability  $\varepsilon$  or vacuum with probability  $1 - \varepsilon$ . The state of incident light arriving at two receivers of pair  $k$  is  $\rho_k = (1 - \varepsilon)|\text{vac}\rangle\langle\text{vac}| + \varepsilon|\Psi_k\rangle\langle\Psi_k|$ , where

$$|\Psi_k\rangle = \frac{1}{\sqrt{2}}(|01\rangle + e^{i\phi_k}|10\rangle), \quad \phi_k \approx 2\pi \frac{L_k}{\lambda} \theta.$$

Suppose the detector has a dark count rate  $d$ , an imperfect detection efficiency  $\xi$ , and the channel has a transmittance  $\eta_k$ . After transmitting through the channel, the state becomes to

$$\rho'_k = (1 - \varepsilon')|\text{vac}\rangle\langle\text{vac}| + \varepsilon'|\Psi_k\rangle\langle\Psi_k|,$$

where  $\varepsilon' = \varepsilon\eta_k$ . After transmitting through the beam-splitter, the state is

$$\rho'_k = (1 - \varepsilon')|\text{vac}\rangle\langle\text{vac}| + \varepsilon'|\Psi'_k\rangle\langle\Psi'_k|,$$

where

$$|\Psi'_k\rangle = \frac{1}{2}(1 - e^{i\phi_k})|01\rangle + (1 + e^{i\phi_k})|10\rangle$$

Considering the dark count rate  $d$  and imperfect detection efficiency  $\xi$ , we obtain the probability of  $D_a$  silent and  $D_b$  clicking:

$$p_k = (1 - \varepsilon')(1 - d)d + \varepsilon'(1 - d)\xi \frac{1}{2}(1 - \cos \phi_k).$$

We detect totally  $M_k$  time-windows and observe the event of detector  $D_a$  silent and  $D_b$  clicking for  $m_k$  times. Taking the asymptotic approximation  $p_k \approx \frac{m_k}{M_k}$  we obtain

$$\cos \phi_k \approx 1 - 2 \frac{\frac{m_k}{M_k} - (1 - \varepsilon')(1 - d)d}{\varepsilon'(1 - d)\xi} := q_k. \quad (\text{S18})$$

Setting  $\frac{\pi}{2}$  phase shift for  $S$ , we observe the event of detector  $D_a$  silent and  $D_b$  clicking for  $\bar{m}_k$  times in total  $\bar{M}_k$  time-windows. Replacing  $\{m_k, M_k, \phi_k\}$  by  $\{\bar{m}_k, \bar{M}_k, \phi_k + \frac{\pi}{2}\}$  in Eq. (S18), we have

$$\sin \phi_k \approx 2 \frac{\frac{\bar{m}_k}{\bar{M}_k} - (1 - \varepsilon')(1 - d)d}{\varepsilon'(1 - d)\xi} - 1 := \bar{q}_k. \quad (\text{S19})$$

So we obtain  $\hat{\phi}_k = \frac{1}{2}(\cos^{-1} q_k + \sin^{-1} \bar{q}_k) \bmod 2\pi$ .

### III. Angular precisions of classical and existing quantum telescope

For a classical telescope with diameter  $D$ , the probability distribution of detected angle  $\theta_c$  is well-approximated by Gaussian function with the standard deviation

$\sigma(\theta_c) = \frac{\sqrt{2}\lambda}{\pi D}$  [3]. Taking Central-limit Theorem with 3 standard deviations and  $M_t$  incident photons, we formula the following precision of detected angle

$$\delta\theta_c := \frac{3\sigma(\theta_c)}{\sqrt{M_t}} = \frac{3\sqrt{2}\lambda}{\pi D\sqrt{M_t}}.$$

For a fair comparison, we assume the same initial crude information about angle  $\theta$  for existing quantum telescopes [1–4] and our method, i.e.,  $\theta \in [0, \theta_{\max}]$  and  $\theta_{\max}$  is a known value. Existing quantum telescopes with baseline  $l$  can detect the phase value in the range  $\phi \in [0, 2\pi)$  and the angle value in the range  $\theta \in [0, \lambda/l)$  [3]. Given the range above, the optimal length of baseline is  $l = \lambda/\theta_{\max}$ . Then the precision of existing quantum telescope is [3]:

$$\delta\theta_Q := \frac{3\sigma(\theta_Q)}{\sqrt{M_t}} \geq \frac{3\lambda}{2\pi l\sqrt{M_t}} = \frac{3\theta_{\max}}{2\pi\sqrt{M_t}},$$

where  $M_t$  is the incident photon number.

#### IV. An alternative method for single-star target

We show an alternative method to determine the value of  $\phi_0$  by using the data  $\{q_k, \bar{q}_k | k = 0, 1, \dots, K\}$  from Eq. (12). We still set the baseline to be  $L_k = 2^k L_0$  and have  $\phi_{k+1} = 2\phi_k$ . We introduce the phase-slide function

$$\psi_k(\omega) = (\phi_k + \omega) \bmod 2\pi. \quad (\text{S20})$$

Applying Eqs. (S18) and (S19), we have

$$\sin \psi_k(\omega) \approx q_k \sin \omega + \bar{q}_k \cos \omega.$$

Maximizing  $\sin^2 \psi_k(\omega)$  over  $\{\omega\}$ , we get two set of solutions

$$\begin{cases} \sin \omega_k = q_k, & \cos \omega_k = \bar{q}_k, \\ \Rightarrow \omega_k = \frac{1}{2}(\sin^{-1} q_k + \cos^{-1} \bar{q}_k), \\ \sin \psi_k(\omega_k) \approx 1. \end{cases}$$

or

$$\begin{cases} \sin \omega_k = -q_k, & \cos \omega_k = -\bar{q}_k, \\ \Rightarrow \omega_k = \frac{1}{2}(\sin^{-1}(-q_k) + \cos^{-1}(-\bar{q}_k)), \\ \sin \psi_k(\omega_k) \approx -1. \end{cases} \quad (\text{S21})$$

We choose anyone of these two solutions and define the binary value  $b_k$ : if  $\sin \psi_k(\omega_k) > 0$  ( $< 0$ ), then  $b_k = 0$  ( $\pi$ ).

*Theorem 2:* Asymptotically, given  $\omega_k, b_k, \omega_{k+1}$  and  $\psi_{k+1}(\omega_{k+1})$ , the value of  $\psi_k(\omega_k)$  is determined by the following form

$$\psi_k(\omega_k) = b_k + \frac{1}{2}[(\psi_{k+1}(\omega_{k+1}) + 2\omega_k - \omega_{k+1}) \bmod 2\pi].$$

*Proof:* We rewrite  $\psi_k(\omega_k)$  in the following form consisting of  $\psi_k(\omega_k) \bmod \pi$  and  $b_k := \psi_k(\omega_k) - \psi_k(\omega_k) \bmod \pi$

$$\begin{aligned} & \psi_k(\omega_k) \\ &= b_k + \psi_k(\omega_k) \bmod \pi \\ &= b_k + (\phi_k + \omega_k + \frac{\omega_{k+1}}{2} - \frac{\omega_{k+1}}{2}) \bmod \pi \\ &= b_k + [(\phi_k + \frac{\omega_{k+1}}{2}) \bmod \pi + \omega_k - \frac{\omega_{k+1}}{2}] \bmod \pi \\ &= b_k + (\frac{(\phi_{k+1} + \omega_{k+1}) \bmod 2\pi}{2} + \omega_k - \frac{\omega_{k+1}}{2}) \bmod \pi \\ &= b_k + \frac{1}{2}[(\psi_{k+1} + 2\omega_k - \omega_{k+1}) \bmod 2\pi]. \end{aligned} \quad (\text{S22})$$

Here  $\omega_{k+1}$  and  $\psi_{k+1}$  are obtained in the last iteration so only  $b_k$  is unknown and  $b_k = 0$  or  $\pi$ . From Eq. (S22) we also have if  $\sin \psi_k(\omega_k) > 0$  ( $< 0$ ), then  $b_k = 0$  ( $\pi$ ).  $\square$

*Method 1:* Given the detected data  $\{q_k, \bar{q}_k | k = 0, \dots, K\}$  in Eq. (12), we calculate  $\{\omega_k, b_k | k = 0, \dots, K\}$  from the content around Eq. (S21). Applying Theorem 2, we determine the value of  $\psi_k(\omega_k)$  iteratively

$$\psi_K(\omega_K) \Rightarrow \psi_{K-1}(\omega_{K-1}) \Rightarrow \dots \Rightarrow \psi_1(\omega_1) \Rightarrow \psi_0(\omega_0).$$

The initial condition is also given by Eq. (S21): if  $\sin \psi_K(\omega_K) \approx 1$  ( $-1$ ), then  $\psi_K(\omega_K) \approx \frac{1}{4}$  ( $\frac{3}{4}$ ). Applying Eq. (S20), we can get  $\phi_0$  from  $\psi_0(\omega_0)$

$$\phi_0 = (\psi_0(\omega_0) - \omega_0) \bmod 2\pi.$$

With the same precision as Eq. (14), we numerically simulate the failure probability of Method 2

$$\epsilon = P(|\tilde{\phi}_0 - \phi_0| > \frac{\pi}{2^{K+1}}).$$

where  $\tilde{\phi}_0$  is the result obtained from Method 1. Same to Sec. III in the main text, we calculate the failure probability with  $K = 14, M = 1, 4$  and  $7$  as shown in Fig. (S6). We find that the failure probability in Fig. (S6) is lower than that in Fig. 4.

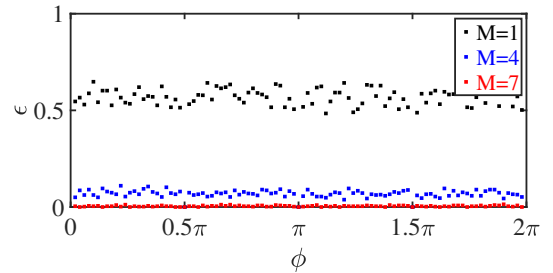


FIG. S6. The failure probability  $\epsilon$  changes with  $\phi$  for detecting single-star target by applying Method 2. We take  $M_k = \bar{M}_k = M$  for every  $k$ . The failure probability for the red data points is around 0.0046, about 63% of 0.0073 in Fig. 4. Each data point is obtained by averaging 500 samples.